ELSEVIER

FEBS Letters 344 (1994) 55–60

FEBS 13967

FEBS LETTERS

Conformational study of three endothelin antagonists with ^{1}H NMR at low temperature and molecular dynamics

Patricia Verheyden[a,*], Ivo Van Assche[b], Marie-Hélène Brichard[b], Thierry Demaude[b], Ingrid Paye[b], Alain Scarso[b], Georges Van Binst[a]

[a]*Department of Organic Chemistry, Vrije Universiteit Brussel, Pleinlaan, B-1050 Brussel, Belgium*
[b]*UCB Bioproducts, Chemin du Foriest, B-1420 Braine-L'Alleud, Belgium*

Received 28 January 1994; revised version received 29 March 1994

Abstract

The conformations of three endothelin antagonists, a cyclic pentapeptide, a linear tripeptide and a linear hexapeptide, are compared by ^{1}H NMR and molecular dynamics. The three analogues have a Leu and a DTrp side chain which are oriented parallel, and an acidic group next to the DTrp residue.

Key words: Endothelin; Antagonist; BQ123; ^{1}H NMR; MD

1. Introduction

Endothelin-1, a bicyclic 21 residue peptide, is one of the most potent vasoconstrictors known today. It was first isolated in 1988 from the culture supernatant of porcine endothelial cells [1]. In the search for the regions of ET-1 responsible for receptor binding and biological activity the study of antagonists is of great importance. Several antagonists are reported in the literature [2–5], as well small peptidic as organic antagonists are known, most of them discovered by random screening.

We report the study by ^{1}H NMR of three of those antagonists in methanol at low temperature.
BQ123 cyclo(Leu-DTrp-DAsp-Pro-DVal)
hexapeptide AC-DTrp-Leu-Asp-Ile-Ile-Trp
BQ610 hexahydroazepinocarbonyl-Leu-DTrp(CHO)-DTrp

The conformation of BQ123 has been studied previously in acetonitrile/water at 293 K by Pelton et al. [6]. The authors found a β turn around Leu-DTrp and a γ' turn around Pro. The same conformation was also found in DMSO, CD_3CN, TFE/water and glycol/water at room temperature [7,8]. A comparison of the molecular modelling structures of ET-1 and BQ123 [9] reports about analogy between BQ123 and ET-1 [6–8].

We have chosen to do the NMR measurements at low temperature since the lowering of the temperature reduces the molecular mobility and a stable conformation could dominate in the equilibrium. In addition at low temperature the viscosity increases, which, for molecules of this size, increases the intensity of the NOESY crosspeaks, resulting in more information concerning the conformation.

2. Materials and methods

NMR samples were prepared by dissolving the peptides (1.55 mg BQ610, purchased from Neosystem Laboratories, 1 mg BQ123, purchased from Peninsula Laboratories and 2 mg hexapeptide, synthesised) in 0.5 ml. of a 0.1% TFA solution (pH ± 2). After lyophilisation and drying over P_2O_5 under vacuum the peptides were dissolved in 0.4 ml. CD_3OH (99.9% D, MSD isotopes). Spectra were recorded on a Bruker AMX 500 spectrometer equipped with an X32 computer and a Eurotherm temperature control unit. 1D spectra were measured at different temperatures between 193 K and 303 K. The 1D spectra were recorded with 8K data points, which were multiplied by a Gaussian filter and zero filled to 32K data points before Fourier transformation. The 2D spectra were measured at 193 K and at 203 K. 2D NOESY [10] and HOHAHA [11] spectra in the phase sensitive mode were recorded using the TPPI method [12]. 2D HOHAHA spectra were recorded by spin-locking during 20 or 60 ms with an MLEV17 [13] sequence using a 10 kHz spin-lock field preceded and followed by 2.5 ms trim pulses. 2D NOESY spectra were measured with mixing times of 100, 200 and 400 ms. Since careful examination of the NOESY spectra gave no indications of spin diffusion at 200 ms, NOE intensities at this mixing time were used in the calculations. The solvent signal was suppressed using presaturation during the relaxation delay and, for the NOESY spectra, also during the mixing time. Typically 256 FID's of 2K data points, 32 scans each were accumulated. In ω_2 the data were processed using a $\pi/3$ shifted sine bell window, followed by Fourier transformation and phase correction. In ω_1 the resulting FID's were zero filled to 2K data points, multiplied by a $\pi/3$ shifted sine bell window, Fourier transformed and phase corrected. A polynomial base line correction in both dimensions was performed. Spectral references were determined at different temperatures in a separate experiment using a methanol-d_3 sample with internal TMS. Restrained molecular dynamics were performed on a Silicon Graphics Iris 4D 310 GTXb using the Insight and Discover software from Biosym. The cvff (consistent valence force field) potential function was used. The NOE's observed at 200 ms were

*Corresponding author. Fax: (32) (2) 6413 304.

SSDI 0014-5793(94)00352-V

classified as being strong, medium or weak,. corresponding to upper limits used in the calculations of 3, 4 and 5 Å The lower limit was set to 1.8 Å. A forcing potential of 100 kcal·mol^{-1}·Å^2 was used. The number of contraints used is summarized in Table 1. Each restrained MD run comprised 100 ps dynamics at 900 K, saving a structure every 5 ps. The resulting 20 structures were cooled down to 300 K during 5 ps of dynamics, and were then energy minimised resulting in 20 low energy structures.

3. Results and discussion

3.1. BQ123 cyclo(Leu-DTrp-DAsp-Pro-DVal)

The spin systems were assigned using 2D HOHAHA and 2D NOESY spectra. The chemical shifts are summarised in Table 2. The small $^3J_{NH\text{-}C^\alpha H}$ for Leu (3.9 Hz), combined with the strong d_{NN} NOE, the weak $d_{\alpha N}$ NOE between DTrp and DAsp, and the medium NOE between NH DAsp and C^αH Leu are characteristic for a β_{II} turn over Leu-DTrp (Table 3).

The intermediate value of $\Delta\delta_{NH}/\Delta T$ for Asp (−4.2 ppb/K) indicate that this turn is partly stabilised by a H-bridge. The $\Delta\delta_{NH}/\Delta T$ for Val, however, is very small (−0.5 ppb/K), This amide proton is probably involved in a H-bridge with C = O DAsp, stabilising a γ-turn around Pro.

A combination of $^3J_{C^\alpha H\text{-}C^\beta H}$ coupling constants at 303 K and NOE's allowed the determination of the side chain orientations at room temperature. At 303 K the sidechains of Leu, DTrp and DVal were found to prefer the gauche$^+$ orientation, while for the DAsp sidechain the trans orientation is predominant. At low temperatures coupling constants can not be measured due to line broadening. The high field shift of Leu C^γH at low temperature is remarkable: a difference in chemical shift of 0.6 ppm is observed between 303 K (0.85 ppm) and 193 K (0.24 ppm). Together with the NOE's between H_1 DTrp and Leu $C^\gamma H/C^\delta H/C^{\delta'}H$ this shows the close proximity of the Leu and DTrp sidechains. This proximity however is incompatible with χ_1 Leu = 60 and χ_1 DTrp = 60 as determined at 303 K. A molecular dynamics simulation using all the observed NOE's as restraints was used to study the conformation further. Only one of the 20 resulting structures had a constraint violation which is larger than 0.1 Å (1 Å) and was discarded. The remaining 19 low energy structures are very well defined, the RMS differences of the backbone were smaller than 0.1 Å (Table 1). The energy of those structures varied less than 3 kcal/mol. The observed dihedrals are summarised in Table 4. The sidechain orientation of the Leu and DTrp sidechains that is in accordance with the observed NOE's at 193 K is respectively gauche$^-$ and gauche$^+$. This differs from what is observed at room temperature. We can conclude that the sidechain orientation of Leu changes from gauche$^+$ to gauche$^-$ upon lowering of the temperature. This change in orientation brings the Leu and DTrp sidechains close to each other as is observed by NOE's and the high field shift of the Leu $C^\gamma H/C^\delta H/C^{\delta'}H$. Probably this orientation is the most stable since it appears at low temperature.

Table 1
Number of constraints used in the MD runs of the different peptides, mean energies and RMS differences of the resulting structures

	BQ123	Hexapeptide	BQ610
Number of constraints			
Intraresidual	41	27	18
Sequential	21	22	16
Long range	2	5	0
Mean energy (kcal/mol)			
Van Der Waals	52 (± 1.7)	62 (± 2.2)	74 (± 2.4)
Forcing	3.3 (± 0.2)	0.4 (± 0.1)	2.3 (± 0.4)
Coulomb	0.87 (± (0.05)	1.4 (± 0.1)	−0.45 (± 0.09)
RMS differences (Å)			
Backbone	0.1 (± 0.06)	0.9 (± 0.4)	0.8 (± 0.3)
All	1.1 (± 0.3)	1.6 (± 0.4)	3.0 (± 1.0)

Table 2
Chemical shifts (in ppm) in cyclo(Leu-DTrp-DAsp-Pro-DVal) in CD_3OH at 193 K

Residue	NH	C^αH	$C^\beta H/C^{\beta'}H$	Others
Leu	9.16	3.92	1.32/1.16	$C^\beta H/C^{\beta'}H$ 1.37/1.28, $C^\gamma H$ 0.24, $C^\delta H/C^{\delta'}H$ 0.77/0.53
DTrp	9.45	4.58	3.58/2.86	H_1 10.49, H_2 7.14, H_4 7.62, H_5 6.99, H_6 7.07, H_7 7.31
DAsp	8.31	5.20	2.96/2.50	
Pro		4.91	2.31/1.78	$C^\gamma H/C^{\gamma'}H$ 2.04, $C^\delta H/C^{\delta'}H$ 3.49/3.32
DVal	7.62	4.06	1.78	$C^\gamma H_3/C^{\gamma'}H_3$ 0.96/0.91

3.2. AC-DTrp^{16}-Leu^{17}-Asp^{18}-Ile^{19}-Ile^{20}-Trp^{21}

2D HOHAHA and 2D NOESY spectra were used for the assignment, the chemical shifts are summarised in Table 5. The numbering of this analogue is chosen so that corresponding residues in ET-1 and the hexapeptide have the same number.

At room temperature most $^3J_{NH\text{-}C^\alpha H}$ coupling constants have values indicative of averaging (7.4–8.1 Hz). The temperature dependence of the amide proton chemical shift is large (>6 ppb/K) except for Ile^{19} NH (−1.8 ppb/K) (Table 6). The small value observed for this amide proton indicates that Ile^{19} NH is part of a intramolecular H-bridge. On the basis of the observed NOE's it was not clear to which C = O this H-bridge is oriented. The NOE's between DTrp^{16} and Trp^{21} (Trp^{21} H_1 to Trp^{16} C^βH, Trp^{21} H_7 to Trp^{16} C^βH, Trp^{21} H_7 to Trp^{16} NH) show that the hexapeptide adopts a cyclic conformation. Restrained molecular dynamics indicates the possibility of a turn around Ile^{17}-Asp^{18} stabilised by a H bridge between Ile^{19} NH and DTrp^{16} C = O. MD was performed based on the NOE's observed at low temperature, no coupling constants were included since they were deter-

Table 3
Sequential NOE's observed for BQ123 cyclo(Leu-DTrp-DAsp-Pro-DVal) in CD_3OH at 193 K in a 2D NOESY spectrum with a 200 ms mixing time

	$d_{\alpha N}$	$d_{\beta N}$	$d_{\gamma N}$	d_{NN}	$^3J_{NH\text{-}C^\alpha H}$ (243 K)	$\Delta\delta_{NH}/\Delta T$ (ppb/K)	$^3J_{C^\alpha H\text{-}C^\beta H}/^3J_{C^\alpha H\text{-}C^{\beta'} H}$ (303 K)
Leu	+++	+	+		3.9	−6.0	3.0/6.0
DTrp	+			+++	7.6	−8.8	11.4/3.6
DAsp	$\alpha\delta\delta$				8.7	−4.2	4.2/10
Pro	+++						
DVal	+++		+	+	10.2	−0.5	10

(+, weak NOE; +++, strong NOE)

Table 4
Mean backbone and χ_1 dihedrals as observed in 100 ps restrained MD for BQ123

	$<\phi>$ (± S.D.)	$<\psi>$ (± S.D.)	$<\chi_1>$
Leu	−75° (± 3°)	142° (± 7°)	g^-
DTrp	75° (± 5°)	44° (± 5°)	g^+
DAsp	102° (± 7°)	−107° (± 7°)	$t/g^+/g^-$
Pro	−78° (± 6°)	94° (± 6°)	30°/−30°
DVal	83° (± 6°)	−110° (± 5°)	t/g^+

Table 5
Assignment of the chemical shifts of AC-DTrp-Leu-Asp-Ile-Ile-Trp in CD_3OH at 193 K

Residue	NH	$C^\alpha H$	$C^\beta H/C^{\beta'} H$	Others
				Ac 2.00
DTrp[16]	9.15	4.44	3.2/3.2	H_1 10.9, H_2 6.98, H_4 7.58, H_5 7.05, H_6 7.10, H_7 7.31
Leu[17]	8.78	4.02	1.32/1.16	$C^\gamma H$ 1.56, $C^\delta H/C^{\delta'} H$ 0.40/0.03
Asp[18]	8.68	4.68	3.01/2.88	
Ile[19]	7.71	3.99	1.62	$C^\gamma H_3$ 0.9, $C^\gamma H$ 0.2, $C^\delta H_3$ 0.76
Ile[20]	8.68	4.06	1.72	$C^\gamma H_3$ 0.9, $C^\gamma H$ 0.35, $C\delta H_3$ 0.9
Trp[21]	9.20	4.46	3.4/3.05	H_1 10.82, H_2 7.25, H_4 7.6 H_5 7.05, H_6 7.12, H_7 7.46

Table 6
Sequential NOE's observed for AC-DTrp-Leu-Asp-Ile-Ile-Trp in CD_3OH at 193 K in a 2D NOESY spectrum with a 200 ms mixing time

	$d_{\alpha N}$	$d_{\beta N}$	d_{NN}	$^3J_{NH\text{-}C^\alpha H}$ (303 K)	$\Delta\delta_{NH}/\Delta T$ (ppb/K)
DTrp	+++	++	++		
Leu	+	+		7.9	−6.8
Asp	++	+		7.8	−6.1
Ile	+			8.1	−1.8
Ile	+++	++	+	7.4	−9.5
Trp				6.1	−9.8

(+, weak NOE; ++, medium NOE; +++, strong NOE)

mined at a different temperature. No constraint violations larger than 0.05 Å were observed. Although the molecule is linear the structures resulting from molecular dynamics all have a cyclic conformation with the peptide bond Ile[20]-DTrp[21] close to the acetyl group of DTrp[16], and the C-terminal acidic group oriented away from it, to the outside of the molecule (Fig. 2). The average dihedrals resulting from the restrained molecular dynamics run, are summarised in Table 7. Clearly this analogue is much more flexible than the cyclic pentapeptide BQ123, especially the C-terminal part shows conformational mobility, as can be seen from the large fluctuations of the dihedrals. The RMS differences of the low energy structures are thus also large (Table 1). In this molecule the sidechains of DTrp[16] and Leu[17] are close to each other in all the low energy conformations, with their χ_1 dihedrals respectively in the trans and the gauche$^-$ conformation.

3.3. BQ610: hexahydroazepinocarbonyl-Leu-DTrp(CHO)-DTrp

The spin systems were assigned using 2D HOHAHA and 2D NOESY spectra. The chemical shifts are summarised in Table 8. Two distinct sets of crosspeaks are present for DTrp(CHO) in the ratio 2/1, the same ratio is observed in the whole temperature domain studied 303–193K. Both the DTrp(CHO) have sequential $d_{\alpha N}$, $d_{\beta N}$, $d_{\gamma N}$, $d_{\delta N}$ NOE's with a Leu sidechain at the same chemical shift (a second signal is also visible for Leu NH and DTrp[3] H_1 but here the differences in chemical shift are too small to observe the complete set separately). This is caused by the presence of two orientations from the CHO group on DTrp[2]. Conformer 1 in Table 8 is the

Table 7
Mean backbone and χ_1 dihedrals as observed in 100 ps restrained MD for AC-DTrp-Leu-Asp-Ile-Ile-Trp

	$<\phi>$ (± S.D.)	$<\psi>$ (± S.D.)	$<\chi_1>$
DTrp	130/90° (± 8°)	125° (± 5°)	t
Leu	70° (± 7°)	−90° (± 10°)	g^-
Asp	−78° (± 8°)	60° (± 10°)	t/g^+
Ile	−85° (± 5°)	110° (± 15°)	t
Ile	+−90° (± 5°)	very flexible	g^-/t
DTrp	very flexible		g^-

Fig. 1. Stereo view of the superposition of 19 low energy structures of BQ123 resulting from molecular dynamics using the observed NOE's as restraints.

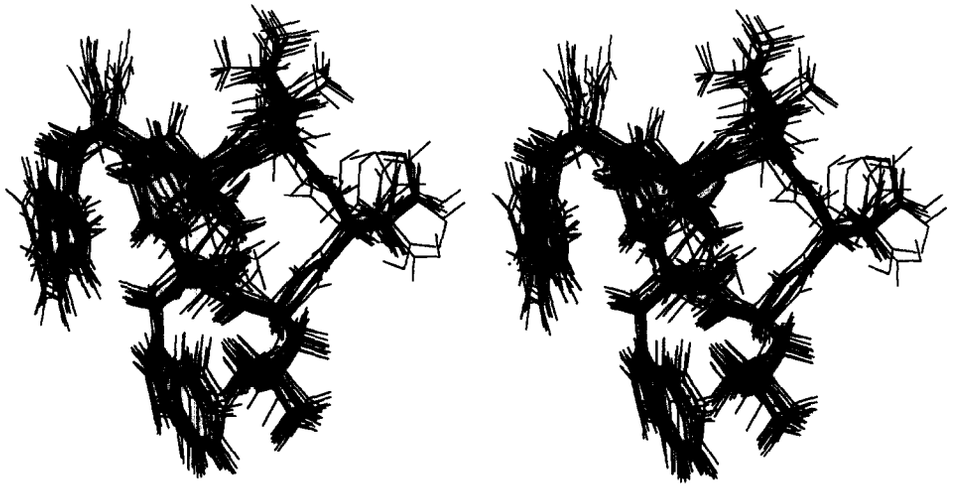

Fig. 2. Stereo view of the superposition of the 20 low energy structures of AC-DTrp-Leu-Asp-Ile-Ile-Trp resulting from molecular dynamics using the observed NOE's as restraints.

Fig. 3. Stereo view of the superposition of the 19 low energy structures of BQ610 resulting from molecular dynamics using the observed NOE's as restraints (for clarity the hydrogen atoms and the sidechain of Trp^3 are omitted).

Table 8
Assignment of the chemical shifts of BQ610 in CD_3OH at 203 K

Residue	NH	$C^{\alpha}H$	$C^{\beta}H/C^{\beta'}H$	Others
Hexahydroazepine				1.48, 1.62, 1.69, 3.23, 3.38, 3.54
Leu[1]	6.49	3.99	1.21	$C^{\gamma}H$, $C^{\delta}{}_3/C^{\delta}H_3$ 0.78/0.61
DTrp[2]				
conformer 1	8.85	4.94	3.41/2.82	CHO 9.11, H_2 7.4, H_4 7.68, H_5 7.35, H_6 7.35, H_7 8.3
conformer 2	9.05	4.92	3.43/2.8	CHO 9.57, H_2 7.37, H_4 7.71, H_5 7.35, H_6 7.35, H_7 7.9
DTrp[3]	9.05	4.56	3.4	H_1 10.8, H_2 7.3, H_4 7.6, H_5 7.05, H_6 7.12, H_7 7.35

most important set of signals. In this conformer the low field shift of DTrp[2] H_7 and the NOE crosspeak between the aldehyde proton and DTrp[2] H_2 indicate that the aldehyde C = O is oriented to the H_7 proton of DTrp. In the second conformer a NOE between the aldehyde proton and DTrp[2] H_7 confirms the reverse orientation of the CHO group. The $\Delta\delta_{NH}/\Delta T$ are large (−10 ppb/K for DTrp[2] and −7 ppb/K for DTrp[3]) for all amide protons which indicates that no H-bridges are present. Coupling constants could not be determined due to the large line width, the observed NOE's are all intraresidual or sequential. Exchange crosspeaks between the amide protons of the two DTrp residues corresponding to position 2 in the peptide are observed in the NOESY spectra at low temperature. Also at room temperature exchange between the two amide protons and between the two aldehyde protons is observed in a ROESY spectrum. NOESY crosspeaks between the aromatic sidechain of DTrp(CHO) and Leu are observed. A molecular dynamics simulation using all the NOE's observed for the most intense set of DTrp(CHO) signals was performed. Only one of the 20 resulting structures had a constraint violation which is larger than 0.1 Å (1.1 Å), this structure was not included in further interpretations. The resulting structures show that the molecule is very flexible. RMS differences are very large (Table 1) for this molecule and the backbone dihedrals are very variable (Table 9). The part Leu-DTrp(CHO) is the least flexible part of the molecule. Although two different orientations of the DTrp(CHO) sidechain are observed, this sidechain and the Leu sidechain are always in close proximity. DTrp[3], however, is very flexible, the backbone dihedrals vary in a large range and the sidechain adopts all possible orientations. In Fig. 3 the sidechain of Trp[3] is not shown.

Table 9
Mean backbone and χ_1 dihedrals as observed for BQ610 in 100 ps restrained MD

	$<\phi>$ (± S.D.)	$<\psi>$ (± S.D.)	$<\chi_1>$
Leu	70° (± 2°)/−80° (± 10°)	160° (± 10°)	g^-
DTrp	160/110° (± 2°)	−110° (± 25°)	g^-/g^+
DTrp	−135° (± 35°)		$g^-/g^+/t$

4. Conclusion

Since all the observed NOE's are compatible with one structure as well for the cyclic pentapeptide cyclo(Leu-DTrp-DAsp-Pro-DVal) as for the linear hexapeptide AC-DTrp-Leu-Asp-Ile-Ile-Trp it is very likely that, in methanol at low temperature, one conformation is predominant for those two peptides. The smaller linear tripeptide however is much more flexible in the conditions used here.

When Figs. 1, 2 and 3 are compared the most striking analogy is the proximity of the Leu and DTrp residues in the three analogues. In the linear hexapeptide however the backbone is reversed compared to the two other antagonists. The three molecules have an acidic group which is situated approximately on the same position relative to the Leu and DTrp sidechains. For the cyclic BQ123 this is the DAsp sidechain COOH, for the linear tripeptide and hexapeptide the C-terminal COOH function. The fact that also non-peptidic molecules are found to be antagonists indicate that the presence of a peptidic backbone is not necessary for biological activity. Those non-peptidic antagonists are less potent than the peptidic antagonists, but they are less flexible which makes them interesting for conformational comparison. The low energy structures of the non-peptidic antagonist Ro 46–2005 [14] for instance also have a hydrophobic and an aromatic group which fit on those of the three peptides studied here. The acidic group is then replaced by a hydroxylgroup. We can conclude that DTrp[16]-Leu[17] of the hexapeptide corresponds to Leu-DTrp of the pentapeptide. Comparison of the three analogues studied here indicate the necessity of a hydrophobic group (here Leu) next to an indole (here the DTrp sidechain) and the presence of an acidic group for biological activity.

Acknowledgements: We would like to thank José C. Martins (Vrije Universiteit Brussel) for the careful reading of the manuscript.

References

[1] Yanagisawa, M., Kurihara, H., Kimura, S., Tomobe, Y., Kobayashi, M., Mitsui, Y. Yazaki, Y., Goto, K. and Masaki, T. (1988) Nature 332, 411–415.

[2] Ihara, M., Fukuroda, Saeki, T., Masaru, N., Kojiri, K., Suda, H. and Yano, M. (1991) Biochem. Biophys. Res. Commun. 178, 132–137.
[3] Ishikawa, K., Fukami, T., Hayama, T., Niiyama, K., Nagase, T., Mase, T., Fujita, K., Kumagai, U., Urakawa, Y., Kimura, S., Ihara, M. and Yano, M. (1991) Proc. 12th Am. Pept. Symp. 812–813.
[4] Cody, W.L., Doherty, A.M., He, J.X., DePue, P.L., Rapundalo, S.T., Hingorani, G.A., Major, T.C., Panek, R.L., Dudley, D.T., Haleen, S.J., LaDouceur, D., Hill, K.E., Flynn, M.A. and Reynolds, E.E. (1992) J. Med. Chem. 35, 3301–3303.
[5] Mast, S.G. and Castaner, R.M. (1992) Current Drug Data Reports 645–655.
[6] Atkinson, R.A. and Pelton, J.T. (1992) FEBS Lett. 296, 1–6.
[7] Krystek, S.R., Bassolino, D.A., Bruccoleri, R.E., Hunt, J.T., Porubcan, M.A., Wandler, C.F. and Andersen, N.H. (1992) FEBS Lett. 299, 255–261.
[8] Reilly, M.D., Thanabal, V., Omecinsky, D.O., Dunbar, J.B., Doherty, A.M. and DePue, P.L. (1992) FEBS Lett. 300, 136–140.
[9] Satoh, T. and Barlow, D. (1992) FEBS Lett. 310, 83–87.
[10] Macura, S., Huang, Y., Suter, D. and Ernst, R.R. (1981) J. Magn. Reson. 43, 259–281.
[11] Braunschweiler, L. and Ernst, R.R. (1983) J. Magn. Reson. 53, 521–528.
[12] Marion, D. and Wüthrich, K. (1983) Biochem. Biophys. Res. Commun. 113. 967–974.
[13] Bax, A. and Davis, D.G. (1985) J. Magn. Reson. 65, 355–360.
[14] Clozel, M., Breu, V., Burri, K., Cassel, J.M., Fishli, G. et al. (1993) 3rd International Conference on Endothelin, Houston, p. 17.